

# The motion of a dipolar spherical particle in homogeneous shear and time-periodic fields

By I. PUYESKY AND I. FRANKEL

Faculty of Aerospace Engineering, Technion - Israel Institute of Technology, Haifa 32000, Israel

(Received 18 October 1996 and in revised form 22 July 1997)

The effects of the intensity and frequency of a time-periodic external field on the rotary motion of a dipolar spherical particle suspended in homogeneous shear are studied with the goal of providing insight into problems concerning the motion of swimming microorganisms and the macroscopic behaviour of ferrofluids. The analysis reveals two modes of motion: convergence of the particle to a global time-periodic attractor, and quasi-periodic motion. The former mode of particle rotation generally appears for sufficiently strong fields. However, asymptotic analysis clarifies that it may occur even for very weak fields as a cumulative result of appropriate resonance interactions.

A sufficient condition for the occurrence of a global time-periodic attractor is established for an external field acting in the plane of shear. Asymptotic results together with numerical evidence indicate that this condition is in fact a necessary condition as well. Making use of this condition we obtain the division of the plane of parameters into domains respectively corresponding to quasi-periodic motion and global time-periodic attractors. The latter domain has the structure of non-intersecting Arnold's tongues. Throughout each, the average frequency of dipole rotation about the vorticity vector is a constant (integral) multiple of the forcing frequency (frequency locking). In the case of quasi-periodic motion, there simultaneously coexist separate domains in orientation space where the rotary motion is locally characterized by different constant rotation numbers. These may assume both rational and irrational values. Potential implications of the distinction between these modes of rotary motion on the characterization of effective (macroscale) ferrofluid properties are briefly discussed.

---

## 1. Introduction

In the presence of an appropriate external field, dipolar microscopic particles suspended in a carrier fluid are subject to an orienting torque tending to align them with the direction of the imposed field. Such particles appear in a wide variety of engineering applications (e.g. ferrofluids) as well as natural phenomena (e.g. the motion of certain microorganisms).

Ferrofluids are suspensions of fine solid single-domain ferromagnetic particles. These ferrofluids have a wide range of engineering uses (e.g. in separation processes, printing, tribology, information display etc., cf. Rosensweig 1985). Under the action of external magnetic fields, these fluids exhibit interesting macroscopic features including antisymmetric stresses, some unique types of hydrodynamic instabilities, and unusual buoyancy relationships. The qualitative explanation as well as quantitative estimates of these phenomena depend upon the appropriate description of the dynamics of the microscopic ferromagnetic particles suspended in the carrier fluid.

The swimming direction of many microorganisms is determined by the presence of an appropriate external field. Thus (cf. the review by Pedley & Kessler 1992), various species of algae possess an asymmetric mass distribution creating a gravitational dipole which makes them swim upwards in still water ('gravitaxis'); some bacteria contain magnetic particles which cause them to move along magnetic field lines ('magnetotaxis').

The motion of a dipolar sphere subject to a steady external field and suspended in a steady homogeneous shear flow was first analysed by Hall & Busenberg (1969) and Brenner (1970*b*) with the goal of calculating the effective rheological behaviour of such a dilute suspension. These analyses were later extended by Brenner & Weissman (1972) and Hinch & Leal (1972) who incorporated the respective effects of strong and weak Brownian rotations on the rheology of the suspension. More recently, Almog & Frankel (1995) analysed the rotary motion of an axisymmetric dipolar particle in simple shear.

The present contribution focuses on the effects of time-periodic external fields on the rotary motion of spherical dipolar particles suspended in steady homogeneous shear. The potential application of an appropriate external forcing as a means of controlling the macroscopic dynamic behaviour of a suspension dates back to the works of Batchelor (1970) and Brenner (1970*a*). Recently, Shliomis & Morozov (1994) and Bacri *et al.* (1995) reported a decrease in the effective viscosity of a ferrofluid under the action of time-periodic magnetic fields. Additionally, Heegaard *et al.* (1996) and Gazeau *et al.* (1996) propose the use of the optical properties of a dilute ferrofluid under the action of a static or an alternating field as a means of measuring local fluid vorticity. The effect of time-varying fields on the motion (in a quiescent fluid) of magnetic bacteria was studied by Steinberger *et al.* (1994). In another work, Jones, LeBaron & Pedley (1994) studied the motion under gravity in steady shear of biflagellate algal cells, the unsteady feature being introduced into the problem through the motion of the flagella (the 'flagellar beat').

Time-dependent problems have been studied both theoretically and experimentally in a series of papers by Szeri, Wiggins & Leal (1991), Szeri, Milliken & Leal (1992) and Szeri & Leal (1993). They, however, considered the rotary motion in general time-dependent shear of torque-free axisymmetric particles. More recently, Ramamohan and various coworkers (Ramamohan *et al.* 1994; Kumar & Ramamohan 1995; and Kumar, Kumar & Ramamohan 1995) presented results of numerical simulations concerning the motion in simple shear of dipolar spheroids subject to time-periodic external fields.

Our goal in the present paper is to analyse the respective effects on particle rotary motion of the external field intensity and the forcing frequency. In particular we seek to determine whether or not a global time-periodic attractor exists. A brief outline of this paper now follows. In the next section we formulate the equations of motion for a single dipolar particle suspended in an unbounded Newtonian fluid. Asymptotic results in the respective limits of weak field and weak shear are obtained in §3 and §4. In §5 the modes of motion found in the preceding section are illustrated for non-asymptotic parameters. In §6 we discuss the conditions for the appearance of time-periodic attractors and describe the corresponding motion. The other mode of quasi-periodic motion is studied in §7. Remarks on the significance of the occurrence of a stable time-periodic attractor in determining the macroscopic behaviour of a dilute suspension appear in §8. Finally, the Proposition underlying the discussion in §6 is substantiated in the Appendix.

## 2. The equation of motion

We consider the rotary motion of a permanent dipolar spherical particle in a steady homogeneous shear flow in the presence of an unsteady external field. We focus on the case of a zero-mean time-periodic field with a period  $T$ , an amplitude  $|F|$ , and acting in the direction parallel to the constant unit vector  $\hat{F}$

$$\mathbf{F}(t) = |F|f(t)\hat{F}. \quad (2.1)$$

Normalizing the time variable with respect to the period  $T$  of the external field, the time-periodic scalar function  $f(t)$  satisfies for all  $t$

$$f(t+1) = f(t), \quad \int_t^{t+1} f(t_1) dt_1 = 0, \quad \text{and} \quad |f(t)| \leq 1. \quad (2.2a-c)$$

Neglecting particle- and fluid-inertial effects and assuming hydrodynamic quasi-steadiness, the (dimensionless) angular velocity of the dipolar sphere

$$\Omega = \delta \hat{\omega} + \gamma f(t) \mathbf{e} \times \hat{F} \quad (2.3)$$

consists of two contributions respectively resulting from the viscous torque due to the shear flow acting to rotate the particle in the direction of the unit vector  $\hat{\omega}$  parallel to the undisturbed fluid vorticity, and the external torque tending to align the unit vector  $\mathbf{e}$  attached to the particle dipolar axis with the direction  $\hat{F}$  of the external field. In (2.3) the dimensionless parameters

$$\delta = |\omega|T, \quad \text{and} \quad \gamma = \frac{q|F|T}{8\pi\mu a^3} \quad (2.4a, b)$$

appear where  $|\omega|$  is one half of the magnitude of the undisturbed fluid vorticity,  $\mu$  denotes the fluid viscosity,  $q$  is the strength of the permanent dipole moment, and  $a$  is the particle radius. The parameters  $\delta$  and  $\gamma$  represent the ratios of  $T$  and the time scales respectively associated with the undisturbed fluid rotation,  $|\omega|^{-1}$ , and the rotation of the suspended particle resulting from the action of the external field,  $8\pi\mu a^3/q|F|$ .

The instantaneous orientation of the dipolar sphere is completely specified by the unit vector  $\mathbf{e}$  (figure 1) whose dimensionless rate of change is  $\dot{\mathbf{e}} = \Omega \times \mathbf{e}$ . Making use of (2.3) we obtain the equation of rotary motion

$$\dot{\mathbf{e}} = \delta \hat{\omega} \times \mathbf{e} + \gamma f(t)(\mathbf{I} - \mathbf{e}\mathbf{e}) \cdot \hat{F}. \quad (2.5)$$

When  $\mathbf{e}$  is parametrized in terms of the polar angles  $(\theta, \phi)$  defined<sup>†</sup> in figure 1, one obtains the pair of first-order nonlinear differential equations

$$\dot{\theta} = \gamma f(t) (\sin \theta_F \cos \theta \cos \phi - \cos \theta_F \sin \theta), \quad (2.6a)$$

and

$$\dot{\phi} = \delta - \gamma f(t) \sin \theta_F \frac{\sin \phi}{\sin \theta}, \quad (2.6b)$$

in which  $\theta_F$  denotes (cf. figure 1) the angle between the directions of the undisturbed fluid vorticity and the external field. The above system is invariant under the transformation

$$\theta_{F_1} = \pi - \theta_F, \quad \theta_1 = \pi - \theta, \quad \phi_1 = \phi, \quad (2.7)$$

<sup>†</sup> The azimuthal direction of the external field in the plane of shear ( $\theta = \frac{1}{2}\pi$ ) is obviously insignificant. Thus, without loss of generality, the angle  $\phi$  is measured from the projection of  $\hat{F}$  on that plane.

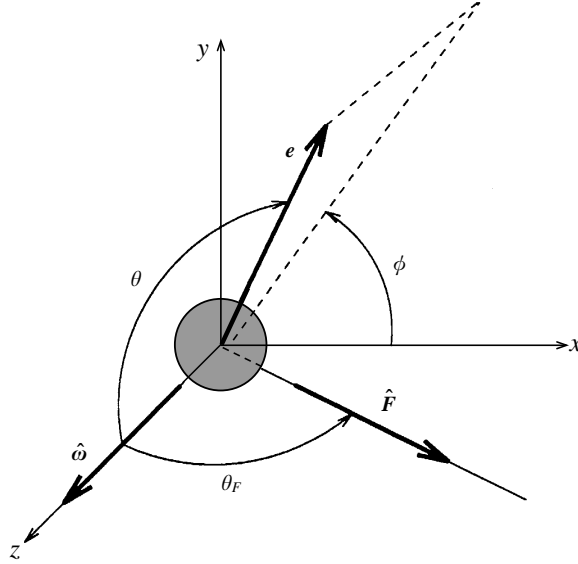


FIGURE 1. Definition of particle's dipole orientation  $e \equiv (\theta, \phi)$  and the angle  $\theta_F$  between  $\hat{\omega}$  and  $\hat{F}$ . The Cartesian frame of reference is chosen so that  $\hat{\omega}$  is parallel to the  $z$ -axis and  $\hat{F}$  lies in the  $(x, z)$ -plane.

thus particle trajectories for  $\theta_{F_1}$  are obtained by reflection with respect to the plane of shear. Due to the appearance of the time-dependent external-field intensity in (2.6a), the system is non-autonomous and, in general, cannot be integrated analytically. An exception is the case  $\theta_F = 0$  when the external field is parallel to the fluid vorticity, in which case (2.6a) and (2.6a) are decoupled and their solution corresponding to an initial orientation  $(\theta(0), \phi(0))$  is

$$\tan\left(\frac{\theta}{2}\right) = \tan\left(\frac{\theta(0)}{2}\right) \exp\left[-\gamma \int_0^t f(t_1) dt_1\right], \quad \text{and} \quad \phi = \phi(0) + \delta t. \quad (2.8a, b)$$

It follows from (2.2) that (2.8) describes  $T$ -periodic variations in  $\theta$  superimposed on a constant-rate rotation (with a period  $2\pi/|\omega|$ ) about the vorticity vector. Since no closed-form solutions are obtainable for  $\theta_F \neq 0$ , we proceed to obtain asymptotic approximations in the respective limits of weak external field ( $\gamma \ll 1$ ) and weak shear ( $\delta \ll 1$ ).

### 3. Weak field ( $\gamma \ll 1$ )

We assume the regular expansions

$$\theta(t) = \sum_{n=0}^{\infty} \gamma^n \theta_n(t) \quad \text{and} \quad \phi(t) = \sum_{n=0}^{\infty} \gamma^n \phi_n(t) \quad (3.1a, b)$$

together with the initial conditions

$$\theta_0(0) = \theta(0), \quad \phi_0(0) = \phi(0), \quad \text{and} \quad \theta_n(0), \phi_n(0) = 0, \quad n = 1, 2, \dots \quad (3.2a, b)$$

Substitution into (2.6a) yields a sequence of linear initial-value problems which are solved recursively. In the case of the harmonic external field

$$f(t) = \sin 2\pi t, \quad (3.3)$$

we obtain

$$\theta(t) \cong \theta(0) + \gamma \left\{ \sin \theta_F \cos \theta(0) \left[ \frac{2\pi \cos \phi(0)}{4\pi^2 - \delta^2} - \frac{\cos((2\pi - \delta)t - \phi(0))}{2(2\pi - \delta)} - \frac{\cos((2\pi + \delta)t + \phi(0))}{2(2\pi + \delta)} \right] + \cos \theta_F \sin \theta(0) \frac{\cos 2\pi t - 1}{2\pi} \right\} + O(\gamma^2), \quad (3.4a)$$

and

$$\phi(t) \cong \phi(0) + \left[ 1 + \gamma^2 \frac{\sin^2 \theta_F}{4(4\pi^2 - \delta^2)} + O(\gamma^4) \right] \delta t - \gamma \frac{\sin \theta_F}{\sin \theta(0)} \left[ \frac{2\pi \sin \phi(0)}{4\pi^2 - \delta^2} + \frac{\sin((2\pi - \delta)t - \phi(0))}{2(2\pi - \delta)} - \frac{\sin((2\pi + \delta)t + \phi(0))}{2(2\pi + \delta)} \right] + O(\gamma^2). \quad (3.4b)$$

Thus, provided that  $\delta \neq 2\pi$ , the motion consists of a constant-rate rotation of the dipole about  $\hat{\omega}$  on which weak  $O(\gamma)$  oscillations are superimposed. When  $\theta_F \neq 0, \pi$  the oscillatory motions are quasi-periodic since their respective frequencies  $2\pi \pm \delta$  are in general incommensurable. In the  $O(\gamma^2)$  problem for  $\phi_2$  (whose complete solution is not presented in (3.4)) there appear some secular terms. Removal of these terms (e.g. through the definition of a slow-time variable  $\gamma^2 t$ ) modifies the second (linear in  $t$ ) term on the right-hand side of (3.4b). This modification represents a small shift in the frequency of rotation about the vorticity vector as a result of nonlinear interactions between the respective effects of the shear flow and the (weak) external field.

When  $\delta \cong 2\pi$  the above expansion is non-uniform due to the occurrence of the factor  $(2\pi - \delta)^{-1}$  in some of the (presumed)  $O(\gamma)$  terms. (A similar non-uniformity appears at  $\delta \cong 2\pi$  for an arbitrary  $f(t)$  owing to our normalization of the time with respect the period  $T$ .) In order to obtain an approximation appropriate for  $\delta \cong 2\pi$ , we define the parameter  $s$  through the relation†

$$\delta = 2\pi + s\gamma. \quad (3.5)$$

Assuming the multiple time-scales expansion

$$\theta = \theta_0(t, \tau) + \gamma \theta_1(t, \tau) + O(\gamma^2), \quad \phi = \phi_0(t, \tau) + \gamma \phi_1(t, \tau) + O(\gamma^2) \quad (3.6a, b)$$

where the slow-time variable is  $\tau = \gamma t$ , we obtain from the leading order of (2.6a)

$$\theta_0 = A(\tau), \quad \text{and} \quad \phi_0 = 2\pi\tau + B(\tau). \quad (3.7a, b)$$

Removal of the secular terms in the  $O(\gamma)$  equations yields a first-order autonomous system for  $A$  and  $B$ . Defining the new variables

$$\tau' = (k \sin \theta_F) \tau, \quad \text{and} \quad B' = B + \frac{1}{2}\pi, \quad (3.8a, b)$$

where the value of the constant  $k$  is determined by the specific functional form of  $f(t)$  (e.g.  $k=1/2$  for the harmonic function (3.3)), we then obtain for  $A$  and  $B'$  the system

$$\frac{dA}{d\tau'} = \cos A \cos B', \quad (3.9a)$$

† One may anticipate such a linear relation by inspection of (3.4). Furthermore, (3.5) is readily verified to represent the distinguished limit process in the present context (cf. Bender & Orszag 1978).

and

$$\frac{dB'}{d\tau'} = \frac{s}{k \sin \theta_F} - \frac{\sin B'}{\sin A}, \quad (3.9b)$$

which is supplemented by the initial conditions

$$A(0) = \theta(0), \quad \text{and} \quad B'(0) = \phi(0) + \frac{1}{2}\pi. \quad (3.10a, b)$$

This system is identical to the system governing the motion of a dipolar sphere in the presence of a *steady* external field acting in the plane of shear (i.e. (2.6a) with  $f(t) = 1$  and  $\theta_F = \frac{1}{2}\pi$ ). The analysis of that problem by Hall & Busenberg (1969) established that (in the present notation) for  $|s/k \sin \theta_F| \leq 1$  a stable node exists at  $A = \frac{1}{2}\pi$  and  $B' = \sin^{-1}(s/k \sin \theta_F)$ . Otherwise the rotary motion of the dipolar sphere is periodic.

In terms of the physical variables of the present problem, we conclude that for the case  $|s/k \sin \theta_F| \leq 1$  there exists a time-periodic attractor† in the plane of shear ( $\theta = \frac{1}{2}\pi$ ). The linear (in  $t$ ) term in (3.7) shows that the frequency of rotation about the vorticity vector is independent of both  $\gamma$  and  $\delta$  (at least up to the order calculated). This implies that convergence to the time-periodic attractor is accompanied by frequency locking. That this indeed is the case is demonstrated in a more general context in § 6.

When  $\delta \cong 2\pi$  the frequency of particle rotation due to fluid shear is approximately equal to the frequency of the external field, i.e. the dipole completes one-half of its rotation about  $\hat{\omega}$  when the external field reverses its sense. Thus, the singularity in (3.4) originates from a resonance interaction between the respective effects of the shear flow and the external field on the rotary motion of the particle. As a result, even a weak field can have a significant cumulative effect at long  $O(\gamma^{-1})$  times.

A similar though possibly weaker effect is expected to occur for the harmonic field (3.3) when  $\delta \cong 2\pi(2n+1)$  ( $n = 1, 2, \dots$ ), i.e. whenever the dipole axis completes  $2n+1$  half-rotations about  $\hat{\omega}$  between successive reversals of the external field. Indeed, the factor  $(6\pi - \delta)^{-1}$  appears in the  $O(\gamma^3)$  terms (not presented in (3.4)) of the expansion (3.1) for the external field (3.3). Furthermore, such singularities already appear in the  $O(\gamma)$  terms for the piecewise-constant field

$$f(t) = \begin{cases} 1, & 0 \leq t < 1/2 \\ -1, & 1/2 \leq t < 1 \end{cases} \quad (3.11)$$

owing to the presence of the component  $\sin(6\pi t)$  in its Fourier decomposition.

In general (cf. figure 8), when  $\gamma = O(1)$  and  $\theta_F \neq \frac{1}{2}\pi$ , time-periodic attractors do not lie in the plane of shear. The above result, namely that  $\theta \rightarrow \frac{1}{2}\pi$  for an arbitrary  $\theta_F (\neq \frac{1}{2}\pi)$ , is therefore apparently paradoxical. However, the  $O(\gamma)$  term in (3.4) is a superposition of contributions of the components of the external field parallel and perpendicular to  $\hat{\omega}$  (respectively proportional to  $\cos \theta_F$  and  $\sin \theta_F$ ). According to (2.8), an external field parallel to  $\hat{\omega}$  gives rise to nutational oscillations independent of the precession resulting from fluid shear. Therefore this component does not participate in the resonance interaction discussed above. Indeed, it is not surprising that the component proportional to  $\cos \theta_F$  appears neither in the singular terms in (3.4) nor in the leading-order multiple-scales equations (3.9b). Thus, to  $O(\gamma)$  the time-periodic

† We use here the term time-periodic attractor (cf. Szeri *et al.* 1991) for an attracting integral curve on which the phase is asymptotically independent of the initial orientation (phase locking). Additionally, this terminology serves to distinguish the present attractor defined in phase and time space from limit cycles appearing in autonomous systems.

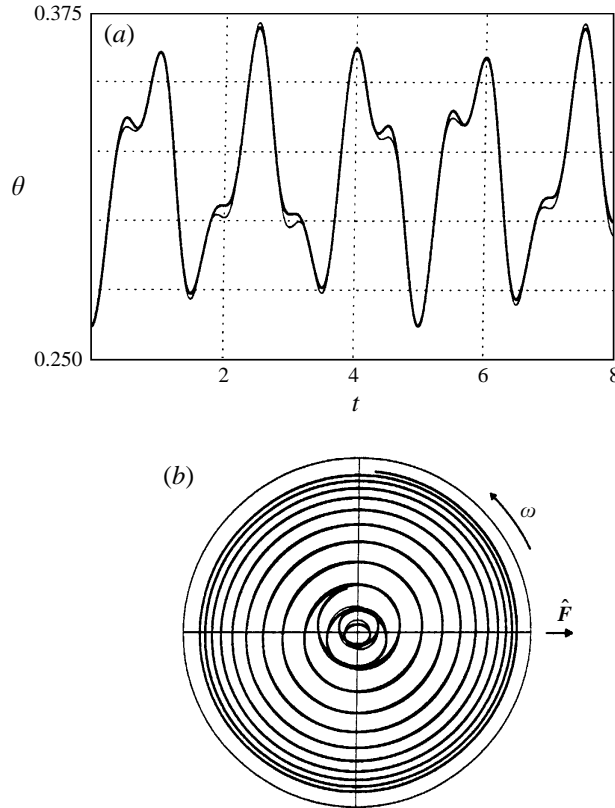


FIGURE 2. Particle motion under harmonic field (3.3),  $\gamma = 0.3$ ,  $\theta_F = \frac{1}{2}\pi$  and initial polar angle  $\theta(0) = \frac{1}{6}\pi$ : —, exact (numerical) results; —, weak-field approximation (3.4a). (a) Variation with time of the polar angle,  $\theta$ , for  $\delta = 2.5$  and initial azimuthal angle,  $\phi(0) = 0$ . (b) Projection on the plane of shear of the particle trajectory for  $\delta = 2\pi$  and initial azimuthal direction  $\phi(0) = \frac{7}{6}\pi$ .

attractor exclusively results from the action of the component of the external field in the plane of shear (as if the other component were entirely missing).

Figure 2 illustrates the foregoing results in the case of a weak ( $\gamma = 0.3$ ) harmonic external field (3.3) acting in the plane of shear,  $\theta_F = \frac{1}{2}\pi$ . Part (a) shows the variation with time of  $\theta$  for  $\delta = 2.5$ , and  $\theta(0) = \frac{1}{6}\pi$ ,  $\phi(0) = 0$ . In agreement with (3.4a) the motion is characterized by the two periods  $2\pi(2\pi + \delta)^{-1} \approx 0.715$ , and  $2\pi(2\pi - \delta)^{-1} \approx 1.66$ , respectively. The ratio between these two periods ( $\approx 2.32$ ) is an irrational number close to  $7/3$  and indeed one may discern during the time interval  $0 \leq t \leq 5$  approximately 3 'long' and 7 'short' periods. The quasi-periodic nature of the motion is evident in that  $\theta(t)$  almost but never exactly reproduces itself. Part (b) of the figure shows the trajectory of the particle in orientation space for  $\delta = 2\pi$ ,  $\theta(0) = \frac{1}{6}\pi$ ,  $\phi(0) = \frac{7}{6}\pi$ , and other parameters the same as before. While in general these paths may be described (for an axisymmetric particle) on the surface of the unit sphere, making use of their symmetry with respect to the 'equator'  $\theta = \frac{1}{2}\pi$ , (2.7), it is sufficient (as well as more convenient) to consider in the present example the projections of particle orbits on the plane of shear. Following a short transient when  $\theta$  decreases, there appears a slow convergence towards the time-periodic attractor at  $\theta = \frac{1}{2}\pi$  (resulting from the cumulative effect of the weak external field). Figure 2 has been

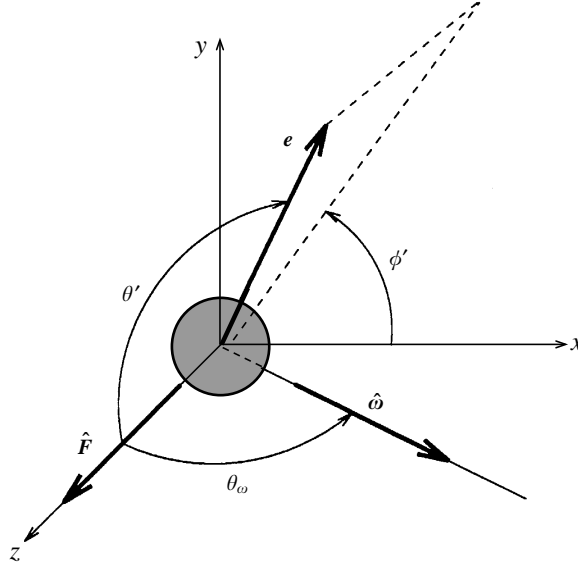


FIGURE 3. Alternative parametrization of the particle's dipole orientation  $e \equiv (\theta', \phi')$  and the angle  $\theta_\omega$  between  $\hat{F}$  and  $\hat{\omega}$ . The Cartesian frame of reference is chosen so that  $\hat{F}$  is parallel to the  $z$ -axis and  $\hat{\omega}$  lies in the  $(x, z)$ -plane.

constructed via numerical integration of (2.6a). However, at the values selected for the parameters, the resulting curves are during most of the time hardly distinguishable from the corresponding asymptotic expressions represented by the thin lines.

In conclusion we note that the foregoing description of the rotary motion consisting of small nutational oscillations superimposed on a constant-rate precession about  $\hat{\omega}$  is not restricted to the limit  $\gamma \ll 1$ . Rather, provided that  $\theta_F \cong \frac{1}{2}\pi$ , this motion takes place whenever the characteristic time of particle rotation associated with the external field is large in comparison with the other time scales of the problem,  $T$  or  $|\omega|^{-1}$ , i.e. when  $\gamma \ll 1$  or  $\gamma \ll \delta$ . Indeed, for  $\delta \gg 1$ , one obtains an asymptotic expansion in powers of  $\gamma/\delta$  which is essentially in agreement with (3.4). This extension does not apply when  $\cos \theta_F = O(1)$  because, as mentioned earlier, the component of the external field acting parallel to the vorticity vector does not directly interact with the fluid shear. As such, this component may, for  $\gamma \cong O(1)$  or larger, induce large  $\theta$  oscillations (cf. (2.8)) irrespective of the ratio  $\gamma/\delta$ . Finally, we note that (3.4) is singular for  $\sin \theta(0) = 0$  too. While this is apparently associated with the parametrization of  $e$  in terms of  $(\theta, \phi)$ , the discussion of the quasi-periodic motion in a more general context (§7) clarifies that (3.4) is genuinely non-uniform when the initial particle orientation is nearly parallel to  $\hat{\omega}$  (i.e.  $\sin \theta(0) \cong O(\gamma)$ ).

#### 4. Weak shear ( $\delta \ll 1$ )

In this case it is convenient to parametrize the vector  $e$  in terms of  $\theta'$ , the polar angle between  $e$  and  $\hat{F}$ , and  $\phi'$ , the azimuthal angle in the plane perpendicular to the external field (figure 3). In terms of these we obtain from (2.5) the equations of motion

$$\dot{\theta}' = -\gamma f(t) \sin \theta' - \delta \sin \theta_\omega \sin \phi', \quad (4.1a)$$

and

$$\dot{\phi}' = -\delta \sin \theta_\omega \frac{\cos \phi'}{\tan \theta'} + \delta \cos \theta_\omega, \quad (4.1b)$$

in which  $\theta_\omega (= -\theta_F)$  denotes the polar angle measured from  $\hat{F}$  to  $\hat{\omega}$ . In the absence of shear, the particle's dipole oscillates in the plane defined by  $\hat{F}$  and the initial orientation of the particle. The introduction of a steady shear, however weak, will have a cumulative effect which will make the particle slowly drift out of that plane. Anticipating this singular behaviour in the limit  $\delta \rightarrow 0$ , we assume the multiple-scales expansions

$$\theta' = \theta_0(t, \tau) + \delta \theta_1(t, \tau) + O(\delta^2), \quad \phi' = \phi_0(t, \tau) + \delta \phi_1(t, \tau) + O(\delta^2) \quad (4.2a, b)$$

wherein the slow-time variable is  $\tau = \delta t$ . In accordance with the above description, substitution of (4.2) into (4.1) yields at the leading order

$$\tan\left(\frac{\theta_0}{2}\right) = \tan\left(\frac{A(\tau)}{2}\right) \exp\left[-\gamma \int_{t_0}^t f(t_1) dt_1\right], \quad \text{and} \quad \phi_0 = B(\tau), \quad (4.3a, b)$$

which indeed show that on the fast time scale  $\phi' = \text{const.}$  and  $\theta'$  is time periodic. The equations governing  $A(\tau)$  and  $B(\tau)$  are obtained via elimination of the secular terms from the  $O(\delta)$  first-order corrections. The resulting system is considerably simplified through an appropriate choice of the value of the redundant parameter  $t_0$  introduced in (4.3a). Specifically, we select  $t_0$  as a solution of the equation

$$\int_0^1 \exp\left[\gamma \int_{t_0}^{t_1} f(t_2) dt_2\right] dt_1 = \int_0^1 \exp\left[-\gamma \int_{t_0}^{t_1} f(t_2) dt_2\right] dt_1. \quad (4.4)$$

It may be verified that for all zero-mean, integrable and periodic functions  $f(t)$ , (4.4) possesses a solution  $0 \leq t_0 \leq 1$  (e.g. for the harmonic function (3.3),  $t_0 = 1/4$  is an appropriate solution). We thus obtain for  $A(\tau)$  and  $B(\tau)$  the autonomous system

$$\frac{dA}{d\tau} = -\alpha \sin \theta_\omega \sin B, \quad (4.5a)$$

and

$$\frac{dB}{d\tau} = -\alpha \sin \theta_\omega \frac{\cos B}{\tan A} + \cos \theta_\omega, \quad (4.5b)$$

supplemented by the initial conditions

$$\tan\left(\frac{A(0)}{2}\right) = \tan\left(\frac{\theta(0)}{2}\right) \exp\left[\gamma \int_{t_0}^0 f(t_1) dt_1\right], \quad \text{and} \quad B(0) = \phi(0). \quad (4.6a, b)$$

In (4.5) the constant parameter

$$\alpha = \int_0^1 \exp\left[\gamma \int_{t_0}^{t_1} f(t_2) dt_2\right] dt_1 \geq 1 \quad (4.7)$$

appears whose value is determined by  $\gamma$  and is the same for all solutions  $t_0$  of (4.4).

The system (4.5) is essentially equivalent to the original system (4.1) in the absence of an external field ( $\gamma = 0$ ). As such we anticipate a periodic solution. Indeed, closed-form integration provides the particle orbits

$$\cos^2\left(\frac{A}{2}\right) \left[ \tan\left(\frac{A}{2}\right) \cos B + \frac{1}{\alpha \tan \theta_\omega} \right] = C \quad (4.8a)$$

and the time dependence

$$\tan\left(\frac{A}{2}\right) = \left[ \frac{2c - b - \operatorname{sgn}(\sin B) \Delta^{1/2} \sin(r\tau + D)}{b + \operatorname{sgn}(\sin B) \Delta^{1/2} \sin(r\tau + D)} \right]^{1/2}. \quad (4.8b)$$

In (4.8b)  $C$  and  $D$  are integration (orbit) parameters determined by the initial conditions (4.6). Also appearing in (4.8b) are the auxiliary constants  $b$ ,  $c$ ,  $\Delta$  exclusively dependent upon  $\alpha$  and  $\theta_\omega$ , and

$$r = [(\alpha^2 - 1) \sin^2 \theta_\omega + 1]^{1/2}. \quad (4.9)$$

Thus,  $A$  and  $B$  are periodic functions of  $\tau$ , the slow-time variable, thereby implying that  $\theta'$  and  $\phi'$  are quasi-periodic functions of  $t$ . It is worthwhile to note that (see (4.8b)) the slow-time variable of the present problem is in fact

$$\tau^* = r\tau = [(\alpha^2 - 1) \sin^2 \theta_\omega + 1]^{1/2} \delta t \quad (4.10)$$

(rather than  $\delta t$ ). Consistency of the foregoing multiple-scales calculation thus requires that  $[(\alpha^2 - 1) \sin^2 \theta_\omega + 1]^{1/2} \delta \ll 1$ . Since  $\alpha$  grows exponentially rapidly for large  $\gamma$ , the latter condition may not be satisfied when  $\gamma$  increases while  $\delta$  is kept fixed. Indeed, it is demonstrated in §6 that the rotary motion is characterized in this limit by a time-periodic attractor.

The above results are illustrated in figure 4 which depicts the rotary motion in the presence of an alternating harmonic external field acting perpendicularly to the fluid vorticity vector ( $\theta_\omega = \frac{1}{2}\pi$ ) when  $\delta = 0.3$ ,  $\gamma = 7$ ,  $\theta'(0) = \frac{5}{6}\pi$ , and  $\phi'(0) = 0$ . Each of the points A, B, ..., correspond to the same instant of time in the three parts of the figure.

Part (a) shows the time variation of  $\theta'$ , the polar angle between the dipole axis and  $\hat{\mathbf{F}}$ . In this part of the figure the respective numerical and asymptotic results are indistinguishable. The two time scales are evident. The rapid oscillations associated with the alternating sense of the external field whose period is  $\approx 1$  are slowly modulated with a period of  $\approx 15.7$ . This value is approximately equal to the period of the motion on the slow time scale which by (4.10) is  $2\pi/\delta\alpha$ . (The corresponding value  $\alpha \cong 1.335$  is obtained from (4.7).) The time variation of  $\phi'$ , the azimuthal angle between the plane of rapid  $\theta'$ -oscillations and the plane of shear, is presented in figure 4(b). The solid thick line is obtained via numerical integration of (4.1) whereas the thin line corresponds to the asymptotic solution (4.8) for  $B(\tau)$ . We see that  $\phi'$  is essentially a function of the 'slow' time variable  $\tau$ . The exact (numerical) solution rapidly oscillates about  $B(\tau)$ , the asymptotic solution. These are, however, small  $O(\delta)$  oscillations which obviously are not accounted for by the  $O(1)$  leading-order multiple-scales solution.

Making use of the symmetry of the motion with respect to the plane of shear ( $(y, z)$  in figure 3), we depict in figure 4(c) the projection of the particle trajectory on this plane. The direction of  $\hat{\mathbf{F}}$  is marked. Again we see that the motion essentially consists of fast  $\theta'$ -oscillations taking place in planes corresponding to constant  $\phi'$ .

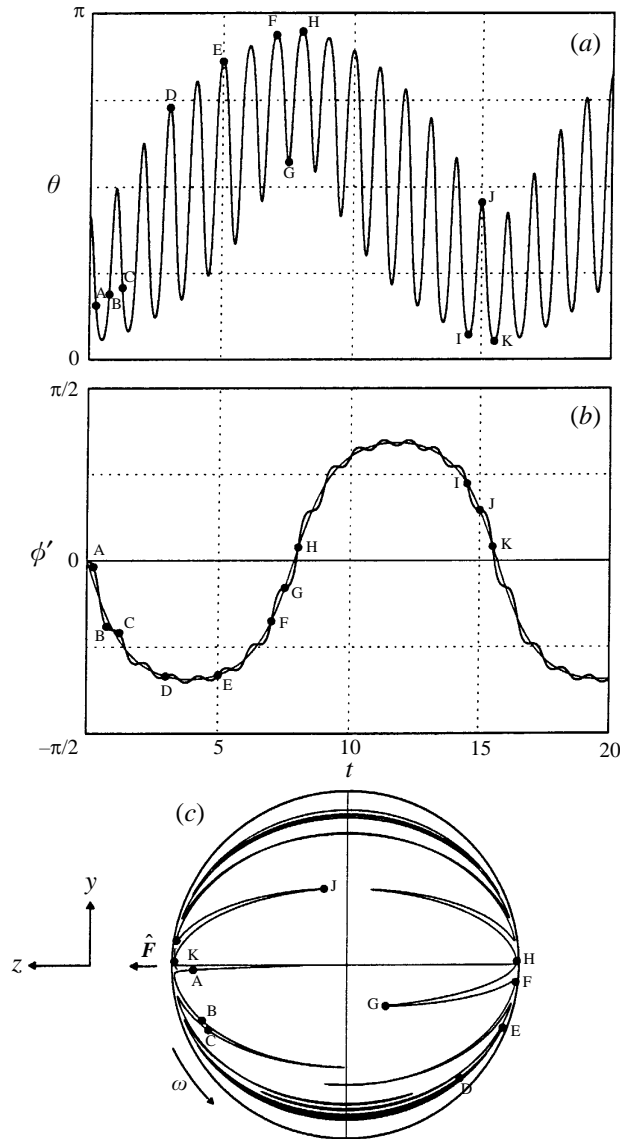


FIGURE 4. Particle motion under harmonic field (3.3),  $\delta = 0.3$ ,  $\gamma = 7$ , and  $\theta_\omega = \frac{1}{2}\pi$ . (a) Variation with time of the polar angle  $\theta'$ . (b) Variation with time of  $\phi'$ : —, exact (numerical) results; ---, weak-shear approximation. (c) Projection of the particle trajectory on the plane of shear. Points A, B, ..., mark the same instants of time in (a)–(c).

On these is superposed a slow  $\phi'$ -drift due to fluid shear. It also appears that in accordance with (4.1b), the more significant variations in  $\phi'$  occur in those portions of the rapid  $\theta'$  oscillations when  $\theta'$  is close to either 0 or  $\pi$ , provided that  $\phi'$  itself is not close to  $\pm\frac{1}{2}\pi$  at the same time (compare, for instance the segments AB and BC in the three parts of the figure). There are on the other hand interim periods (e.g. between  $t \approx 2$  and  $t \approx 6$ , between  $t \approx 10$  and  $t \approx 14$ ) when a number of successive fast  $\theta'$ -oscillations take place with  $\phi'$  remaining nearly constant (see for instance DE). In these periods the slow rotation of the dipole axis about the fluid vorticity

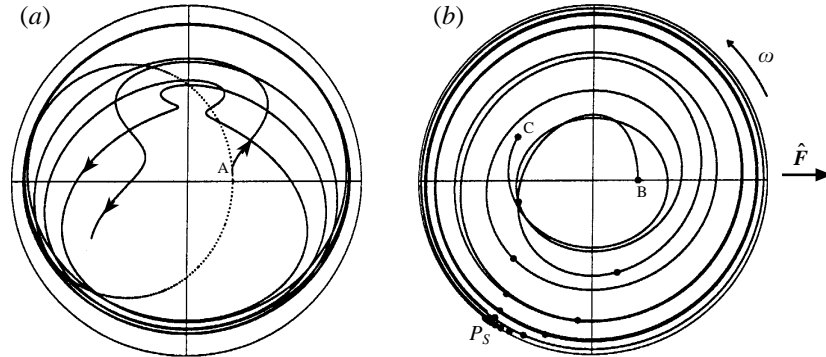


FIGURE 5. Projections on the plane of shear of particle trajectories under harmonic field (3.3) and  $\theta_F = \frac{1}{2}\pi$ . Dots show Poincaré sections. (a) Quasi-periodic motion,  $\gamma = 2.5$ ,  $\delta = 4$ . (b) Time-periodic attractor,  $\gamma = 1$ ,  $\delta = 6$ .

vector progresses mainly through a slow  $\theta'$ -drift between successive oscillations which eventually shift the particle from oscillatory motion between  $\theta' \approx 0$  and some slowly varying maximal value (e.g. I, J, K) to oscillations between some minimal value of  $\theta'$  and  $\theta' \approx \pi$  (like F, G, H). We thus conclude that the slow particle rotation about  $\hat{\omega}$  continuously proceeds through either  $\phi'$ -drift during certain periods or through  $\theta'$ -drift during the rest of the time.

## 5. Modes of rotary motion

The asymptotic results of the preceding sections have shown two modes of rotary motion: convergence to a global time-periodic attractor, and quasi-periodic motion. These two modes are illustrated in figure 5 for non-asymptotic cases (i.e. when neither  $\gamma$  nor  $\delta$  are  $o(1)$ ). Presented are the projections in the plane of shear of particle trajectories in orientation space in the presence of a harmonic external field (3.3) acting in the plane of shear ( $\theta_F = \frac{1}{2}\pi$ ). Solid curves describe the orbits of particles whose respective initial orientations at  $t = 0$  correspond to the indicated points (A, B, and C). Dots mark the corresponding Poincaré sections of the motion at  $t = n$  ( $n = 0, 1, 2, \dots$ ). In part (a) of the figure  $\gamma = 2.5$ ,  $\delta = 4$ . Typical of quasi-periodic motion is the fact that (in the long-time limit) the locus of the Poincaré sections forms a single closed curve. In part (b) of the figure  $\gamma = 1$ ,  $\delta = 6$ . Here the Poincaré sections corresponding to both trajectories converge in the long-time limit to the single periodic point  $P_S$  – a fixed single point of the Poincaré map. In this limit all particles, regardless of their respective initial orientations, will exactly follow the periodic motion of  $P_S$  along the unit circle (phase-locking).

Extensive numerical evidence indicates that the above quasi-periodic motion or convergence to a global time-periodic attractor are the only modes of rotary motion occurring in the present problem. The analysis of the next section is aimed at clarifying how the plane of parameters  $(\gamma, \delta)$  is divided into domains respectively corresponding to these two modes of motion. This classification is important in the context of obtaining the effective suspension properties requisite for the macroscopic description of dilute suspensions of dipolar spheres (cf. § 8).

## 6. Occurrence of time-periodic attractors

Our present goal is to delimit the domains throughout the entire plane of parameters  $(\gamma, \delta)$  where the rotary motion is characterized by convergence to a global time-periodic attractor (TPA). We mainly study the case  $\theta_F = \frac{1}{2}\pi$ , i.e. an external field in the plane of shear, in which case the equations of motion (2.6a) reduce to

$$\dot{\theta} = \gamma f(t) \cos \theta \cos \phi, \quad \text{and} \quad \dot{\phi} = \delta - \gamma f(t) \frac{\sin \phi}{\sin \theta}. \quad (6.1a, b)$$

As noted above (cf.(2.7) *et seq.*), for  $\theta_F = \frac{1}{2}\pi$  the motion is symmetric about the plane of shear. It is, therefore, sufficient to consider the motion on the upper unit hemispherical surface  $0 \leq \theta \leq \frac{1}{2}\pi$ . Moreover, unless otherwise stated, the following description is restricted to the projection of the motion on the plane of shear  $(x, y)$ .

The asymptotic results of the preceding sections together with numerical results indicate that the way in which the system approaches the time-periodic attractor (when it exists) may depend on both the parameters  $(\gamma, \delta)$  and the particle initial orientation  $e_0 = (\theta(0), \phi(0))$  and is not necessarily monotonic. This feature makes it difficult to verify convergence to a TPA. It thus seems insufficient to follow the motion during a short time interval (e.g. a single period). Rather, one needs to describe the long-time limit of the rotary motion corresponding to arbitrary initial conditions. Lacking a closed-form analytical solution to (6.1), we are led to consider Poincaré maps corresponding to ‘sections’ of the motion at the discrete instants of time  $t = n$  ( $n = 0, 1, 2, \dots$ ), rather than continuously follow the rotary motion of the particle.

Consider now the locus at  $t = 0$  of all points within the unit circle which after a single period retain their respective  $\theta$  values, i.e. for each of these points  $\theta(1) = \theta(0)$ . Subsequent analysis focuses on cases when this locus forms a continuous simple curve whose end points A and B lie on the unit circle. Such a curve AB divides the unit circle into a pair of simply-connected domains. (These features may be ascertained analytically in some examples (cf. §6.2). Moreover, numerical results indicate that the locus of  $\theta(1) = \theta(0)$  indeed possesses the above topological properties for any periodic zero-mean  $f(t)$  throughout most of the  $(\gamma, \delta)$ -plane.) When AB does not pass through the origin of the  $(x, y)$ -plane, we denote by U the domain which is respectively bounded by AB and the unit circle and does not include the origin. The complementary domain is denoted by  $\bar{U}$ . At  $t = 1$  the whole curve AB will have moved to  $A'B'$  such that the new end points  $A'$  and  $B'$  remain on the unit circle (since from (6.1a)  $\dot{\theta} = 0$  for  $\theta = \frac{1}{2}\pi$ ). Furthermore the properties of the equations of motion (2.6a) ensure that the transformation from  $(\theta_0, \phi_0)$  at  $t_0$  to  $(\theta, \phi)$  at the time  $t$  is a topological mapping (i.e. a one-to-one mapping such that the forward and inverse transformations are continuous, cf. Coddington & Levinson 1955). Thus  $A'B'$ , the image of AB, remains a continuous simple curve which similarly divides the unit circle into a pair of simply-connected domains S (which does not include the origin) and its complementary  $\bar{S}$ . (Obviously, when AB does not pass through the origin the same is true for its image  $A'B'$ .) Figure 6 illustrates the above-defined curves AB and  $A'B'$  and domains U and S (shaded) for the case of the harmonic field (3.3) and  $\gamma = 2$ ,  $\delta = 4$ . (The actual construction of the curves AB and  $A'B'$  is discussed in §6.1.) Also depicted for future reference are the projections on the plane of shear of trajectories starting at  $t = 0$  at the points C, D, and E.

In accordance with our earlier statement at the very beginning of this section, we now make use of the above definitions to formulate general conditions (for  $\gamma$  and  $\delta$  not necessarily small) for convergence of the rotary motion to a global time-periodic

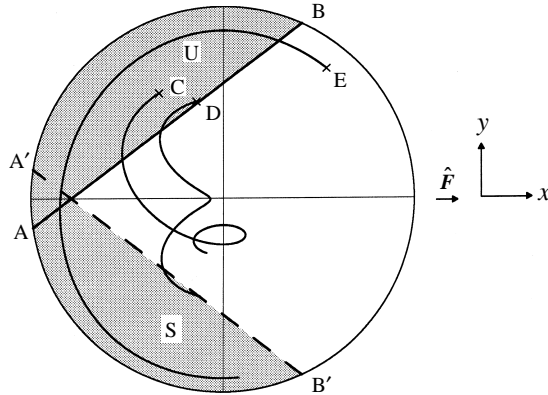


FIGURE 6. The line AB and its image A'B' defining the (shaded) domains U and S. Also presented are the projections on the (x, y)-plane of paths respectively traversed during a single period by the particles starting at C, D, and E. The picture has been drawn for the harmonic field (3.3) and  $\gamma = 2$ ,  $\delta = 4$ .

attractor represented by a periodic point – a fixed point of the Poincaré map. The main results are stated in the following:

**PROPOSITION** *In cases when the domain U at  $t = 0$  is mapped onto  $\bar{S}$  at  $t = 1$  (and  $\bar{U}$  onto S), and provided that*

$$U \cap S = \emptyset, \tag{6.2}$$

then (i)

$$\lim_{n \rightarrow \infty} \theta(n) = \frac{1}{2} \pi, \tag{6.3}$$

and (ii) on the unit circle ( $\theta = \frac{1}{2} \pi$ ) only two periodic points exist: A stable point  $P_S$  on the arc  $A'B' \in S$  and an unstable point  $P_U$  on the arc  $AB \in U$ . The azimuthal angles respectively corresponding to each of these points satisfy

$$\phi_P(n + 1) - \phi_P(n) = 2\pi k, \tag{6.4}$$

wherein the value of  $k = 1, 2, \dots$  is uniquely determined by the parameters  $(\gamma, \delta)$ .

In addition to establishing convergence to a time-periodic attractor, the Proposition enables characterization of the rotary motion on the unit circle. This is provided in terms of the rotation number

$$\rho = \lim_{t \rightarrow \infty} \frac{\phi(t)}{2\pi t} \tag{6.5}$$

(Arnold 1983) representing the long-time average frequency of particle rotation about the vorticity vector. By (6.4)

$$\rho = k \quad (k = 1, 2, \dots), \tag{6.6}$$

wherein the specific value of the integer  $k$  is, for a given  $f(t)$ , uniquely determined by the values of the parameters  $(\gamma, \delta)$  (see (A 1) *et seq.* in the Appendix).

This Proposition is established in the Appendix. An outline of the argument is sketched here. We first show that during a single period  $(0, 1)$  of the external field each particle initially located within  $\bar{U}$  (U) moves to S ( $\bar{S}$ ) with  $\theta$  increasing (decreasing). (See for example the particle trajectories respectively starting at E and C in figure 6.) From this together with the condition (6.2) follows (i). We then proceed to establish

that for all  $\delta > 0$  the sense of motion on the unit circle is such that  $\phi(1) > \phi(0)$ . From this in conjunction with (6.2) and continuity of the transformation during a single period, existence of periodic points is demonstrated. Finally, we verify that  $d\phi(1)/d\phi(0) \geq 1$  for  $\phi(0)$  on  $\text{arc}AB \in U$  and  $d\phi(1)/d\phi(0) \leq 1$  for  $\phi(0)$  on  $\text{arc}\bar{A}\bar{B} \in \bar{U}$  where equality may only apply at a finite number of isolated points. This result serves to substantiate uniqueness and stability (or instability) of the periodic points.

The above Proposition reduces the problem at hand (i.e. verifying convergence to a TPA) to the mapping of the unit circle over just a single period (e.g. between  $t = 0$  and  $t = 1$ ). This mapping directly yields the locus of all points for which  $\theta(1) = \theta(0)$ . The division of the unit circle into respective pairs of simply-connected domains  $U, \bar{U}$  and  $S, \bar{S}$  as well as the transformation  $U \rightarrow \bar{S}$  and  $\bar{U} \rightarrow S$  are thereby readily ascertained, and it is easily examined whether (6.2) is satisfied. For any given combination of the parameters  $(\gamma, \delta)$  and an arbitrary zero-mean periodic  $f(t)$ , the requisite mapping may be effected numerically. However, the usefulness of the Proposition manifests itself most clearly when  $f(t)$  possesses certain symmetry properties in which cases the construction of  $AB$  and hence implementation of the Proposition are significantly facilitated.

### 6.1. Symmetry considerations

Consider  $f(t)$  which is antisymmetric with respect to  $t = 1/2$ , i.e.

$$f(t) = -f(1 - t). \tag{6.7}$$

(Both the harmonic (3.3) and the piecewise-constant (3.11) fields satisfy (6.7).) In these cases the system (6.1) is invariant under the transformation

$$\theta_1 = \theta, \quad \phi_1 = -\phi, \quad \text{and} \quad t_1 = 1 - t. \tag{6.8}$$

From this invariance we conclude that the trajectory traced by a particle during the time interval  $(0, 1)$  is symmetric relative to the  $x$ -axis if the particle is located on this axis at  $t = 1/2$ . Thus, a point such as  $D$  in figure 6, whose initial orientation at  $t = 0$  is  $(\theta_0, \phi_0)$  will move to  $(\theta_0, -\phi_0)$  at  $t = 1$  retaining its original  $\theta$ -value. Consequently, the curve  $AB$  may be constructed through the mapping over a half-period of the diameter of the unit circle which at  $t = 1/2$  coincides with the  $x$ -axis (instead of the above-mentioned mapping of the entire unit circle). The line thus obtained as the image of that diameter is necessarily a simple continuous curve which divides the unit circle into the pair of simply-connected domains  $U$  and  $\bar{U}$ . Furthermore, from the general features of the transformation represented by the solution of (6.1) together with the symmetry property (6.8), it is easily shown that indeed each  $e \in U$  at  $t = 0$  transforms to  $e' \in \bar{S}$  at  $t = 1$  and each  $e \in \bar{U}$  at  $t = 0$  moves to  $e' \in S$  at  $t = 1$ . Obviously the resulting curves  $AB$  and  $A'B'$  are symmetrically disposed with respect to the  $x$ -axis (cf. figure 6). The condition (6.2) is satisfied provided that  $AB$  does not cut the  $x$ -axis. Finally, we note that in both figures 6 and 10 the respective curves  $AB$  and  $A'B'$  (obtained for the harmonic field) appear in fact as straight chords of the unit circle. It is readily verified that  $AB$  and  $A'B'$  are likewise straight for the piecewise-constant field. While it is not obvious what is the general class of functions  $f(t)$  for which  $AB$  are straight, we emphasize that the above proposition makes no use of this feature.

### 6.2. An example

We now apply the above proposition to the case of the piecewise-constant field (3.11). The situation during each half-period is similar to the corresponding steady problem

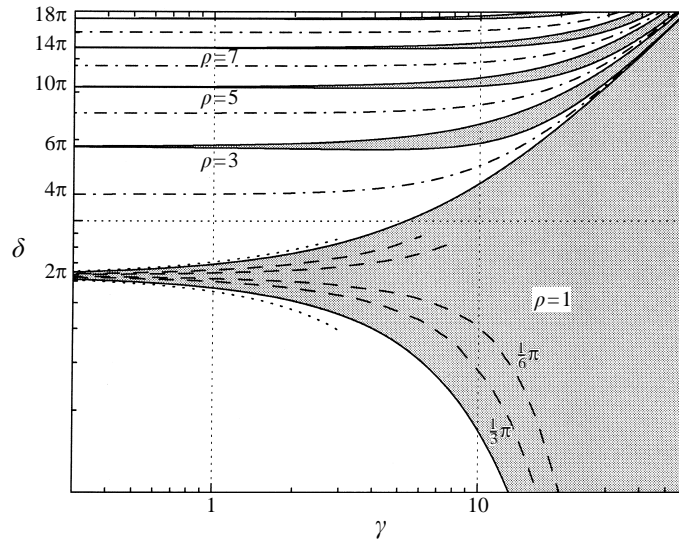


FIGURE 7. Division of the plane of parameters for the piecewise-constant field (3.11) and  $\theta_F = \frac{1}{2}\pi$ . Shading denotes domains of time-periodic attractors corresponding to the indicated values of  $\rho$ : —,  $\gamma_L$  and  $\gamma_U$ ;  $\cdots$ , weak-field ( $\gamma \ll 1$ ) approximations to  $\gamma_L$  and  $\gamma_U$  for  $\rho = 1$ ;  $\cdots\cdots$ , globally periodic motion; - - - -, boundaries of the domain of time-periodic attractor corresponding to  $\rho = 1$  and  $\theta_F = \frac{1}{3}\pi, \frac{1}{6}\pi$ .

in which the external field is time independent. The rotary motion in this steady problem is governed by a single parameter  $\beta = \delta/\gamma$ . Thus (Hall & Busenberg 1969; Brenner 1970*b*; Hinch & Leal 1972), when  $\beta < 1$  the rotary motion is characterized by convergence to a stable equilibrium orientation, whereas for  $\beta > 1$  the motion is periodic about a centre. Making use of the available closed-form solution of the steady problem, it is possible to obtain an analytical expression for the curve AB in the case of a piecewise-constant field. A straightforward calculation (Puyesky & Frankel 1998) then shows that (6.2) is satisfied provided that either

$$\gamma > 4(1 - \beta^2)^{-1/2} \log \left[ \frac{(1 - \beta^2)^{1/2} + 1 - \beta}{(1 - \beta^2)^{1/2} - 1 + \beta} \right] \tag{6.9a}$$

for a given  $\beta < 1$  or, for a given  $\beta > 1$ ,

$$\gamma_L < \gamma < \gamma_U, \tag{6.9b}$$

where

$$\gamma_U, \gamma_L = 4(\beta^2 - 1)^{-1/2} \left[ m\pi + 2 \tan^{-1} \left( \frac{\beta \pm 1}{\beta \mp 1} \right)^{1/2} \right] \quad (m = 0, 1, \dots). \tag{6.9c}$$

The upper and lower signs, respectively corresponding to  $\gamma_U$  and  $\gamma_L$ .

Figure 7 describes the plane of parameters  $(\gamma, \delta)$  for the piecewise-constant field (3.11). The solid lines represent the curves  $\gamma_U$  and  $\gamma_L$  for each  $m = 0, 1, \dots$  as obtained from (6.9). The dashed lines correspond to the indicated values of  $\theta_F \neq \frac{1}{2}\pi$  which are discussed towards the conclusion of this section. Dotted curves represent the weak-field ( $\gamma \ll 1$ ) approximations to  $\gamma_L$  and  $\gamma_U$  for  $m = 0$ .

The foregoing discussion has established that in each of the domains defined by (6.9) (the shaded domains in figure 7) there exists a single stable periodic attractor. The rotary motion is then characterized by the respectively indicated constant values of  $\rho$ , the rotation number (frequency locking). Inasmuch as the piecewise-constant field is symmetric with respect to  $t = 1/4$  too,  $\rho$  only assumes odd integer values (see (A 1) *et seq.*). The rest of the plane of parameters  $(\gamma, \delta)$  outside the shaded domains corresponds, as discussed below, to quasi-periodic motion. While for cases other than piecewise-constant fields no analytical closed-form expressions comparable to (6.9) exist, the domains where (6.2) is satisfied may still be obtained numerically as explained above. Such a calculation has been carried out for the harmonic field (3.3). The resulting picture of the  $(\gamma, \delta)$ -plane is qualitatively very similar to figure 7.

As mentioned above, the motion in the corresponding steady problem is periodic for  $\beta > 1$ . This periodic motion is characterized by the period  $T_P = (2\pi/\gamma)(\beta^2 - 1)^{-1/2}$  which is uniform for all orbits and independent of the initial orientation. In the present unsteady problem if, during the half-period while the external field acts in a constant direction, the particle completes an integral number of rotations along any of these orbits, the rotary motion is globally periodic. This condition yields

$$\gamma_P = 4m\pi (\beta^2 - 1)^{-1/2} \quad (m = 1, 2, \dots), \quad (6.10)$$

which is represented in figure 7 by the dash-dotted curves located between each  $\gamma_U(m - 1)$  and  $\gamma_L(m)$  ( $m = 1, 2, \dots$ ).

When  $\gamma = \gamma_P$  the relation  $\theta(1) = \theta(0)$  is satisfied throughout the unit circle. Obviously, no appropriate definition of the domains U and S is feasible, and the Proposition is inapplicable in this case. Making use of the fact that for the piecewise-constant field (3.11) particle trajectories in orientation space are during each half-period invariant under time shift, it may be verified that the locus of the points for which  $\theta(1) = \theta(0)$  indeed possesses the properties mentioned in the statement of the proposition whenever  $\gamma \neq \gamma_P$ . For cases other than the piecewise-constant field, these properties cannot in general be ascertained by merely applying symmetry considerations.

### 6.3. Additional comments

As mentioned in (ii) following (6.2), when this condition is satisfied there exists a pair of periodic points on the unit circle. Moreover, (6.3) ensures that no such periodic points exist elsewhere (i.e. within the unit circle). When (6.2) is not satisfied AB and A'B' necessarily intersect within the unit circle. For  $f(t)$  satisfying (6.7), by the symmetry relation (6.8), AB and A'B' possess a common point  $P_C$  on the  $x$ -axis. Furthermore, by (6.8), the particle orbit originating from  $P_C$  at  $t = 0$  returns to  $P_C$  at  $t = 1$ , i.e.  $P_C$  is a periodic point (see § 7).

It is interesting whether the present problem admits subharmonic modes characterized by non-integer rational values of  $\rho$ , i.e. whether global time-periodic attractors occur whose period is an integral multiple of that of the external field. Such TPAs, if they exist, will appear as fixed points of the Poincaré mapping based on the appropriate sampling interval  $\Delta t = n(= 2, 3, \dots)$ . We address this issue on the basis of the foregoing discussion (pertaining to sampling interval  $\Delta t = 1$ ) and examine separately the cases when (6.2) is satisfied and is not. In the former case, it is an immediate corollary of the proposition that  $P_S$  represents the unique global TPA for all sampling intervals  $\Delta t = n(= 1, 2, \dots)$ . For  $(\gamma, \delta)$  such that (6.2) is not satisfied and  $f(t)$  satisfying (6.7), the periodic point  $P_C$  mentioned in the preceding paragraph

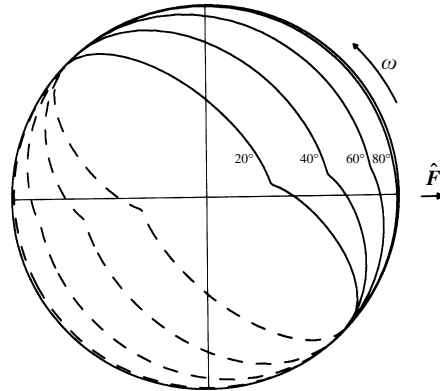


FIGURE 8. Projections on the plane of shear of the periodic attractors corresponding to the harmonic field (3.3),  $\delta = 2$ ,  $\gamma = 30$ , and the indicated values of  $\theta_F$ : —, portions of the orbit lying on the surface of the upper hemisphere ( $0 \leq \theta < \frac{1}{2}\pi$ ); - - - -, projections from the lower hemisphere ( $\frac{1}{2}\pi < \theta \leq \pi$ ).

will appear on the  $x$ -axis in all Poincaré maps. The corresponding curves AB and A'B' of these maps necessarily intersect (at  $P_C$ ), hence  $U \cap S \neq \emptyset$  in all of these maps and, as discussed in the next paragraph, no global TPA is anticipated. Thus, we expect that all global TPAs in the present problem are indeed characterized by integer values of the rotation number (which conclusion is supported by extensive numerical results).

Finally, while the above Proposition constitutes a sufficient condition for the appearance of a stable global time-periodic attractor, numerical evidence suggests that (6.2) is in fact a necessary condition as well. No convergence to a stable periodic orbit has been observed for pairs of  $(\gamma, \delta)$  located outside the domains defined by (6.2). (In a typical integration, the particle is found to execute small rotary fluctuations close to the plane of shear for a large number of periods of the external field (which number increases the closer we approach the bounding curves  $\gamma_L$  or  $\gamma_U$ ), then  $\theta$  sharply decreases returning almost instantaneously to the immediate vicinity of the plane of shear, which pattern recurs quasi-periodically.)

#### 6.4. Time-periodic attractors for $\theta_F \neq \frac{1}{2}\pi$

Extension of the foregoing discussion to cases when the external field does not act in the plane of shear is not obvious. Figure 8 presents numerical results describing the variation of the stable periodic attractors with  $\theta_F$  for the harmonic field (3.3),  $\gamma = 30$ ,  $\delta = 2$ , and the indicated values of  $\theta_F$ . The projections on the plane of shear of the portions of these attractors lying on the surface of the upper unit hemisphere ( $0 \leq \theta < \frac{1}{2}\pi$ ) are marked by the solid lines while the dashed lines correspond to the respective portions on the lower hemispherical surface ( $\frac{1}{2}\pi < \theta \leq \pi$ ). For the given  $f(t)$ , the two portions of each attractor are symmetric with respect to the origin. It is evident that the attractors no longer lie in the plane of shear nor in fact are they planar at all. Thus, it is not obvious whether an appropriate analogue of the curve AB may be defined so as to facilitate the analysis when  $\theta_F \neq \frac{1}{2}\pi$ .

As mentioned above, the dashed curves in figure 7 depict the boundaries of the respective domains in the  $(\gamma, \delta)$ -plane corresponding to  $\rho = 1$  for the indicated values of  $\theta_F$ . With decreasing  $\theta_F$  these boundaries shift to higher values of  $\gamma$ . This trend is in agreement with earlier observations (e.g. the paragraph following (3.11)) that the

contribution to the occurrence of stable periodic attractors of the component of the external field parallel to the vorticity vector is less important than that of the other component.

## 7. Quasi-periodic motion

With the exception of degenerate cases like (6.10) when the entire motion is periodic, the asymptotic results of §3 and §4 together with numerical integration show that whenever  $U \cap S \neq \emptyset$ , the rotary motion is quasi-periodic. Rather than describing the integral curves, we characterize the motion by means of  $\rho$ , the rotation number providing (the long time limit of) the average frequency of the dipole rotation about the vorticity vector. As we shall presently see, unlike the motion when a global time-periodic attractor exists,  $\rho$  is not necessarily constant for a given pair of  $(\gamma, \delta)$  but may depend on the initial orientation.

In the following analysis we restrict ourselves to external fields acting perpendicularly to the vorticity ( $\theta_F = \frac{1}{2}\pi$ ). We start by recalling some general properties of the *one-dimensional* case (corresponding in the present problem to the motion on the unit circle  $\theta = \frac{1}{2}\pi$  for  $\theta_F = \frac{1}{2}\pi$ ). The dynamics of the motion is governed by (6.1b) with  $\theta = \frac{1}{2}\pi$  which may be viewed as a differential equation on the torus possessing no singular points. The Poincaré' map corresponding to this (mapping the unit circle onto itself) is an orientation-preserving diffeomorphism of the circle (Guckenheimer & Holmes 1983; Arnold 1983). Thus, the rotation number exists and is independent of the initial conditions, i.e. its value is exclusively determined by the parameters of the problem  $(\gamma, \delta)$ . Furthermore, if  $\rho$  is irrational the motion is non-periodic and the Poincaré map is dense on the entire unit circle. If on the other hand  $\rho = m/n$  ( $m$  and  $n$  integers) the motion is periodic with a period  $n$ . There are two- (and higher-) dimensional continuous systems which may effectively be represented by one-dimensional orientation-preserving diffeomorphisms (Bohr, Bak & Jensen 1984). If this were the case in the present problem, the above features would still be valid even for initial conditions not on the unit circle  $\theta = \frac{1}{2}\pi$ .

As mentioned in the preceding section, when  $U \cap S \neq \emptyset$  and the external field is antisymmetric with respect to  $t = 1/2$ , there is, by symmetry, at least one periodic point  $P_C$  lying on the  $x$ -axis. It can be verified that for the piecewise-constant field  $P_C$  is unique. Numerical evidence indicates that  $P_C$  is likewise unique for a general  $f(t)$  satisfying (6.7). The rotation number corresponding to (initial conditions at)  $P_C$  is evidently an integer. In contrast with this,  $\rho$  on the unit circle is uniquely determined by the parameters  $(\gamma, \delta)$ . Additionally, as a consequence of  $\phi(1) - \phi(0)$  being a monotonically increasing function of  $\delta$  for  $\theta = \frac{1}{2}\pi$  (cf. the Appendix),  $\rho$  is a continuous non-decreasing function of  $\delta$  there (Guckenheimer & Holmes 1983). The rotation number on the unit circle is thus in general different from that corresponding to  $P_C$ , hence we conclude that  $\rho$  depends on the initial orientation.

Figure 9 describes the variation with  $\delta$  of the quasi-periodic motion for the piecewise-constant field (3.11),  $\gamma = 3$ , and  $\delta = 2$  (a), 4 (b), 9 (c), 12 (d), 15 (e), and 18 (f). Presented are the respective projections onto the plane of shear of domains of initial orientations where  $\rho = \text{const.}$  and equal to the indicated values (the unshaded domains). In each part of the figure two such non-overlapping domains appear: an 'inner' domain bounded by the closed curve  $b_1$ , surrounding the periodic point  $P_C$  (marked by a circle) and an 'outer' domain bounded between the closed curve  $b_2$  (which, in turn, includes  $b_1$  see part (b)) and the unit circle. Within the inner domain

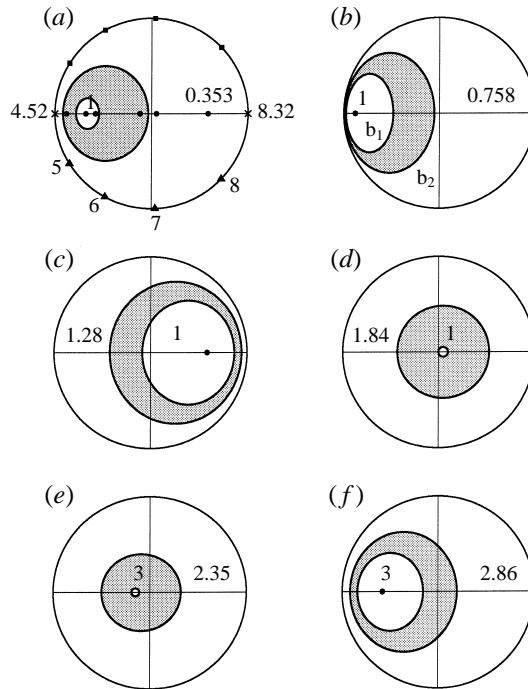


FIGURE 9. Quasi-periodic motion under the piecewise-constant field (3.11) for  $\gamma = 3$ ,  $\theta_F = \frac{1}{2}\pi$ , and  $\delta = 2$  (a), 4 (b), 9 (c), 12 (d), 15 (e), and 18 (f). The closed curves respectively bound the (unshaded) ‘inner’ and ‘outer’ domains of initial orientations for which  $\rho = \text{const.}$  and equal to the indicated values. Also presented in (a) is the variation with  $\delta$  of the type and location of the periodic points:  $\bullet$ ,  $P_C$ ;  $\blacktriangle$ ,  $P_S$ ;  $\blacksquare$ ,  $P_U$ ;  $\times$ , bifurcations.

$\rho$  is equal to an odd integer determined by the motion of the periodic point  $P_C$ . (Here, too, one may readily verify that the additional symmetry of  $f(t)$  with respect to  $t = 1/4$  excludes even integer values of  $\rho$ ). In the outer domain  $\rho < 1$  increases monotonically with  $\delta$  and is determined by the dynamics of the one-dimensional motion on the unit circle.

With increasing  $0 < \delta < 4.52$  (figure 9a,b) the rotation number remains  $\rho = 1$  within the inner domain which moves to the left and expands. In the outer domain  $\rho < 1$  increases monotonically. The intermediate domain gradually shrinks and vanishes altogether at  $\delta = 4.52$  when  $\rho = 1$  throughout the entire orientation space corresponding to the appearance (cf. figure 7) of a global time-periodic attractor, which situation prevails through  $\delta = 8.32$  (cf. (6.9)). For  $8.32 < \delta < 12.91$  (figure 9c,d)  $\rho$  continues to grow in the outer domain and remains at  $\rho = 1$  within the inner domain whose extent diminishes while shifting to the left (towards the origin). For  $12.91 < \delta < 18.44$  (figure 9e,f) we observe trends similar to those described earlier (for  $0 < \delta < 4.52$ ). It is, however, worthwhile to note that  $\rho$  within the inner domain changes discontinuously from  $\rho = 1$  for  $\delta = 12.91^-$  to  $\rho = 3$  for  $\delta = 12.91^+$ . (For  $\delta = 12.91$ , cf. (6.10), the motion is globally periodic.) Finally, at  $\delta = 18.44$  we again have a time-periodic attractor (figure 7) and  $\rho = 3$  for all initial orientations. It is important to emphasize that, unlike the results of the preceding section, the local ‘frequency locking’ observed here for  $0 < \delta < 4.52$  and  $8.32 < \delta < 18.44$  is associated with variation of the initial conditions rather than the parameters of the problem and is not accompanied by phase locking. Additionally, contrary to

one-dimensional orientation-preserving diffeomorphisms, the motion within the inner domain (excluding  $P_C$  itself) is quasi-periodic although  $\rho$  is rational (in fact, an integer).

The foregoing results seem to be inconsistent with the asymptotic results in the limit  $\gamma \ll 1$ . The linear (in  $t$ ) term in (3.4b) shows that  $\rho$  is independent of the initial conditions. This apparent contradiction is resolved by noting that when  $\gamma \ll 1$ ,  $P_C$  lies within an  $O(\gamma)$  distance from the origin, hence  $\sin(\theta(P_C)) = O(\gamma)$ . For this particular initial condition, the factor  $\gamma/\sin(\theta(0))$  appearing in (3.4b) is no longer asymptotically small and the expansion ceases to be uniform. We thus conclude that the asymptotic solution (3.4) corresponds to the outer domain bounded between the unit circle and the curve  $b_2$ . (For  $\gamma \ll 1$  this curve also approaches the origin. However, outside  $b_2$  the factor  $\gamma/\sin(\theta(0))$  in (3.4b) remains asymptotically small.)

Finally, figure 9(a) also presents the variation with  $\delta$  of the type and location of the periodic points. The points  $P_C$ ,  $P_S$ , and  $P_U$  are respectively marked by circles, triangles and squares. The numerical values marked along the circumference of the unit circle denote the values of  $\delta$  respectively corresponding to the bifurcations and the points  $P_S$  shown. (Each of these values of  $\delta$  also correspond to the symmetrically located point  $P_U$ .) The points  $P_C$  marked correspond to the values of  $\delta$  in parts (a–f) of the figure and therefore are not explicitly indicated. For  $0 < \delta < 4.52$  there exists a single periodic point  $P_C$  which, with increasing  $\delta$ , moves leftwards along the  $x$ -axis from  $x \approx -0.62$  (a value which varies with  $\gamma$ ) to  $x = -1^+$ . For  $4.52 < \delta < 8.32$  ( $U \cap S = \emptyset$ ) there simultaneously exist a stable,  $P_S$ , and an unstable,  $P_U$ , periodic points which, with increasing  $\delta$ , move along the unit circle from  $x = -1$  to  $x = 1$ . The bifurcations at  $\delta = 4.52$  and  $\delta = 8.32$  are respectively marked by a cross. For  $8.32 < \delta < 12.91$   $P_C$  moves leftwards along the  $x$ -axis from  $x = 1^-$  to  $x = 0^+$ . At  $\delta = 12.91$ ,  $P_C$  is undefined corresponding to the case of periodic motion. A qualitatively similar description applies to the evolution of the type and location of the periodic points for  $\delta > 12.91$ .

## 8. Concluding remarks

The rotary motion of a dipolar sphere suspended in a homogeneous shear flow and subject to a zero-mean time-periodic external field is either quasi-periodic or converges to a global time-periodic attractor. The latter mode may appear even in cases of weak external field as a result of cumulative resonance interactions between the respective effects of the field and the homogeneous shear.

For an external field perpendicular to fluid vorticity, we have established a sufficient condition for the occurrence of a global time-periodic attractor. Asymptotic results and numerical computations suggest that the established condition is necessary as well. This condition reduces the problem of ascertaining convergence to a global time-periodic attractor to the mapping of orientation space over just a single period of the external field. Symmetry properties of the time variation of this field may considerably simplify the actual calculation.

As mentioned in the introduction, characterization of the specific mode of rotary particle motion is important to the understanding of the motion of microorganisms under the action of a time-periodic field. Additionally, this characterization is essential in the context of the macroscopic behaviour (e.g. rheology, optical properties, etc.) of ferrofluids. The requisite macroscopic description is obtainable (cf. Batchelor 1970; Brenner 1970a) through appropriate averaging with the orientational distribution as the weight function.

When a global time-periodic attractor exists, all particles in the (dilute) suspension will converge to a specific orbit. The resulting ordered distribution is independent of the initial orientations of the particles (as a result of phase locking). However, when the motion is quasi-periodic the dependence upon initial conditions is retained at all times. Furthermore, in this latter case there simultaneously co-exist in orientation space separate domains respectively characterized by different constant (rational and irrational) rotation numbers. It is thus not obvious what time scale needs to be used as a basis for obtaining an appropriate average macroscopic description.

When dealing with sub-micron suspended particles, the orientational distribution may be affected by rotary Brownian diffusion. While the limit of weak diffusion is singular, the present analysis of the deterministic particle motion (i.e. in the absence of diffusion) may still be relevant. Thus, provided that the average attraction of a time-periodic attractor is sufficiently strong, diffusive effects will be negligible outside narrow orientational boundary-layers about the instantaneous dipole orientation within the attractor. These boundary-layers will in turn only slightly modify results concerning the macroscopic behaviour of the suspension (Puyesky & Frankel 1998). When the deterministic motion is quasi-periodic, Brownian rotary diffusion, however weak, will, in the absence of a global attractor, cause the suspended particles to sample at sufficiently long times the entire orientation space. Thus, similarly to the case of periodic motion in the corresponding steady problem (Hinch & Leal 1972b), weak rotary diffusion will have a global effect on the long-time orientational distribution. (Thus, for instance it is expected to render the distribution time-periodic and independent of the initial conditions.) These effects are currently being studied.

The foregoing discussion raises the question of structural stability, i.e. whether or not the motion remains topologically equivalent when the system equations are subject to arbitrary small perturbations. Thus, the above outline of the anticipated effects of weak Brownian rotations indicate that the time-periodic attractor mode is structurally stable, whereas the quasi-periodic motion is not. Preliminary results regarding the rotary motion in the presence of periodic fields of dipolar axisymmetric particles show that the same is true for small deviations from spherical particle geometry. These support the conjecture that the mode of motion characterized by a convergence to a global time-periodic attractor is indeed structurally stable relative to arbitrary small perturbations (e.g. weak interparticle interactions, fluid- and particle-inertial effects, or inhomogeneity of the ambient shear flow (cf. also Szeri *et al.* 1991 and Szeri & Leal 1993.))

This research was supported by the fund for the promotion of research at the Technion. The authors are grateful to Y. Almog for his valuable comments.

#### Appendix. Equations (6.3) and (6.4)

The proposition stated in §6 is concerned with cases when each  $e \in U$  at  $t = 0$  transforms to  $e' \in \bar{S}$  at  $t = 1$  and each  $e \in \bar{U}$  moves to  $e' \in S$ . We first show that during the former transformation  $\theta$  decreases whereas the latter transformation increases  $\theta$ . To this end, we study the images at  $t = 1$  of certain concentric circles within the unit circle at  $t = 0$  (see figure 10). Let  $D$  be the point of  $AB$  for which  $\theta(= \theta_D)$  is the smallest throughout  $AB$ . As mentioned in §6, we study cases when  $AB$  does not pass through the origin, hence  $\theta_D > 0$ . Consider first the circle  $c_1$  passing through the point  $D$ . Since for all  $e \in U$  the polar angle  $\theta \geq \theta_D$ , all points of  $c_1$

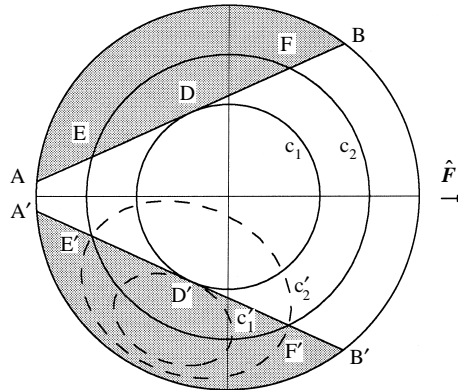


FIGURE 10. The line  $AB$  and its image  $A'B'$  defining the domains  $U$  and  $S$  (shaded). The dashed closed curves  $c'_1$  and  $c'_2$  are the respective images of the circles  $c_1$  and  $c_2$ . The picture has been drawn for the harmonic field (3.3),  $\delta = 5.5$ , and  $\gamma = 2$ .

other than  $D$  necessarily belong to  $\bar{U}$ . Thus (with the exception of  $D'$ , the image of  $D$ , lying on  $A'B'$ ), the closed curve  $c'_1$ , which is the image of  $c_1$ , is entirely within  $S$ . Furthermore, by definition of  $A'B'$  as the image at  $t = 1$  of the curve  $AB$ , for all  $e \in S$  the polar angle  $\theta \geq \theta_D$ . Consequently, each point initially on or within  $c_1$  moves onto or into  $c'_1$  with increasing  $\theta$  (because  $c'_1$  lies outside the circle  $c_1$ ). Let  $c_2$  be any larger concentric circle intersecting  $AB$  at  $E, F$  and  $A'B'$  at  $E', F'$ , respectively. This circle is mapped onto  $c'_2$  which, in turn, includes  $c'_1$ . Moreover, since  $AB$  is the locus of all points within the unit circle for which  $\theta(1) = \theta(0)$ ,  $E'$  and  $F'$  are the *only* points where  $c_2$  intersects its image  $c'_2$ . Consider now  $c_2$  which is only infinitesimally larger than  $c_1$ . The (infinitesimal) arc  $EF \in U$  is transformed to an arc  $\bar{E}'F' \in \bar{S}$  which either is included within  $c_2$  or else is entirely outside it. From continuity, all of this arc remains (infinitesimally) close to the point  $D'$  of  $c'_1$  and therefore necessarily passes within  $c_2$ . The arc  $\bar{EF} \in \bar{U}$  is mapped to arc  $E'F' \in S$ . Similarly to  $\bar{E}'F'$ ,  $E'F'$  either lies entirely outside  $c_2$  or is included within  $c_2$ . Being only infinitesimally larger than  $c_1$ ,  $c_2$  necessarily intersects  $c'_1$  (within  $S$ ). Consequently  $E'F'$  necessarily passes outside  $c_2$  (or else it, too, must intersect  $c'_1$ ). To summarize,  $EF$  moves to  $\bar{E}'F'$  with decreasing  $\theta$  while  $\bar{EF}$  moves to  $E'F'$  with increasing  $\theta$ . We may gradually enlarge the circle  $c_2$  thereby concluding that for any circle  $c_2$  larger than  $c_1$  the arc  $EF \in U$  will be mapped onto arc  $\bar{E}'F' \in \bar{S}$  lying within  $c_2$  (i.e. with  $\theta$  decreasing) and the arc  $\bar{EF} \in \bar{U}$  will move to arc  $E'F' \in S$  outside  $c_2$  (with  $\theta$  increasing) or else we reach a contradiction with either the single-valuedness of the solution of (6.1) or the uniqueness of  $E$  and  $F$  (belonging to  $AB$ ) as the only points on  $c_2$  which preserve their corresponding  $\theta$ -values in the course of transformation between  $t = 0$  and  $t = 1$ . Finally, the above arguments apparently incorporate a tacit assumption regarding uniqueness of the point  $D \in AB$ . It is, however, readily verified that the foregoing results remain valid in cases when the above-defined point  $D$  is not unique or the curve  $AB$  cuts circles like  $c_2$  at more than two points.

When  $\theta(0) \neq \frac{1}{2}\pi$ , then, according to the above, if  $e(0) \in \bar{U}$  then  $e(1) \in S$  and  $\theta(1) > \theta(0)$ . Moreover, since  $U \cap S = \emptyset$ , for all  $n \geq 1$   $e(n) \in \bar{U}$  and  $\theta(n+1) > \theta(n)$ .

† The relative location of the image points  $A'$  and  $B'$  on the unit circle or of  $E', D'$ , and  $F'$  along the curve  $A'B'$  as presented in the figure are dictated by the fact that  $U$  is mapped onto  $\bar{S}$  (and  $\bar{U}$  on  $S$ ) together with the topological nature of the transformation.

Thus  $\theta(n)$   $n = 0, 1, \dots$  is a monotonically increasing sequence bounded from above by  $\frac{1}{2}\pi$ . Consequently, the limit

$$\bar{\theta} = \lim_{n \rightarrow \infty} \theta(n)$$

exists, and it is easily verified that  $\bar{\theta}$  cannot be smaller than  $\frac{1}{2}\pi$ . If, on the other hand,  $e(0) \in U$  then  $e(1) \in \bar{S}$  and  $\theta(1) < \theta(0)$ . Similarly, as long as  $e(n) \in U$   $\theta(n+1) < \theta(n)$ . However, since by definition of the  $U$  domain, for all  $e(n) \in U$   $\theta \geq \theta_D (> 0$ , cf. above), eventually, for  $n$  sufficiently large,  $e(n) \in \bar{U}$ , which thereby substantiates (6.3). A corollary of the foregoing is that (for  $\theta_F = \frac{1}{2}\pi$ ) no periodic orbits can possibly exist outside the plane of shear (i.e. for  $\theta \neq \frac{1}{2}\pi$ ).

We now turn to consider part (ii) of the Proposition in §6. We first examine the orbits  $\phi_1(t)$  and  $\phi_2(t)$  on the unit circle ( $\theta = \frac{1}{2}\pi$ ) respectively corresponding to  $\delta_1 < \delta_2$  and the same function  $f(t)$ , initial value  $\phi(t_0)$ , and parameter  $\gamma$ . Applying an elementary comparison theorem (cf. Birkhoff & Rota 1962), we conclude that  $\phi_2(t) > \phi_1(t)$  for all  $t > t_0$ , thus  $\phi(1) - \phi(0)$  is a monotonically increasing function of  $\delta$ . For  $\delta = 0$  and  $\theta = \frac{1}{2}\pi$  (6.1b) possesses a closed-form solution which, for a zero-mean  $f(t)$ , yields  $\phi(1) - \phi(0) = 0$ . Therefore, for all  $\delta > 0$   $\phi(1) - \phi(0) > 0$ , i.e. the sense of the azimuthal displacement over a single period time interval agrees with that of rotation caused by fluid shear.

From (6.2) together with the preceding result regarding the sense of the motion, as well as the topological nature of the transformation, one may readily verify that the motion of point A during a single period of the external field is such that

$$2\pi(l+1) < \phi_A(1) - \phi_A(0) < 2\pi(l+2), \quad (\text{A } 1a)$$

and

$$2\pi l < \phi_B(1) - \phi_B(0) < 2\pi(l+1), \quad (\text{A } 1b)$$

wherein  $l = 0, 1, 2, \dots$  (These results correspond to the marking of the end points A and B as presented in figure 10, namely such that when traversing the unit circle in the above-mentioned sense, the points appear in the order AA'B'B. This arbitrary specification of A and B involves no loss of generality.) From uniqueness of the solution of the equation of motion (6.1) we conclude that, for a specific  $f(t)$ , the values of the parameters  $(\gamma, \delta)$  determine the integer  $l$  to be substituted in (A 1) (which, in turn, uniquely defines  $k$  in (6.6))<sup>†</sup>. From continuity there exists on the arc  $\overline{AB} \in U$  a point  $P_U$  for which (6.4) is satisfied. Similarly there also exists on the arc  $\overline{A'B'} \in \bar{U}$  a point  $P_S$  for which (6.4) is satisfied. However, since during a single period each  $e \in \bar{U}$  moves to  $e' \in S$ , no periodic point exists in  $\bar{U}$  outside  $S$ . Thus,  $P_S$  is actually on arc  $\overline{A'B'} \in S$ .

Define now the integral

$$I(\theta(0), \phi(0)) = \gamma \int_0^1 f(t) \cos \phi \, dt.$$

<sup>†</sup> Thus, for instance, when  $f(t)$  is antisymmetric with respect to  $t = 1/2$  and symmetric with respect to  $t = 1/4$ , i.e. satisfies (6.7) together with  $f(1/2 - t) = f(t)$ , it may readily be verified that no periodic point completes an even number of rotations around the unit circle during a single period. Only even values of  $l$  may thus appear in (A 1) thereby excluding even values of the rotation number (6.6).

Integration of (6.1a) yields (for  $\theta(0) \neq \frac{1}{2}\pi$ )

$$I = \log \left[ \frac{\tan \left( \frac{1}{4}\pi + \frac{1}{2}\theta(1) \right)}{\tan \left( \frac{1}{4}\pi + \frac{1}{2}\theta(0) \right)} \right]. \quad (\text{A } 2)$$

Making use of some earlier results as well as the fact that  $1 < \tan(\frac{1}{4}\pi + \frac{1}{2}\theta) < \infty$  is monotonically increasing for  $0 < \theta < \frac{1}{2}\pi$ , we conclude that for  $0 \leq \theta(0) < \frac{1}{2}\pi$

$$I \begin{cases} < 0, & e(0) \in U \\ = 0, & e(0) \in AB \\ > 0, & e(0) \in \bar{U}. \end{cases} \quad (\text{A } 3)$$

From continuity of  $\phi(t; e(0))$  with respect to  $e(0)$ , we obtain for  $\theta(0) = \frac{1}{2}\pi$

$$I \begin{cases} \leq 0, & \phi(0) \in \text{arc}AB \\ = 0 & \text{at } A, B \\ \geq 0, & \phi(0) \in \text{arc}\bar{A}\bar{B}. \end{cases} \quad (\text{A } 4)$$

Integration of (6.1b) yields for the pair of orbits  $\phi_1(t)$  and  $\phi_2(t)$  on the unit circle respectively corresponding to initial orientations  $\phi_1(0)$  and  $\phi_2(0)$

$$\frac{\tan \frac{1}{4} (\phi_2(1) - \phi_1(1))}{\tan \frac{1}{4} (\phi_2(0) - \phi_1(0))} = \exp \left[ -\gamma \int_0^1 f(t) \cos \left( \frac{\phi_1 + \phi_2}{2} \right) dt \right]. \quad (\text{A } 5)$$

In the limit  $\phi_2(0) - \phi_1(0) \rightarrow 0$  we obtain

$$\frac{d\phi(1)}{d\phi(0)} = \exp(-I), \quad (\text{A } 6)$$

hence the transformation corresponding to all particle orbits on the unit circle during a single period of the external field satisfies

$$\frac{d\phi(1)}{d\phi(0)} \begin{cases} \geq 1, & \phi(0) \in \text{arc}AB \\ = 1 & \text{at } A, B \\ \leq 1, & \phi(0) \in \text{arc}\bar{A}\bar{B} \end{cases} \quad (\text{A } 7)$$

when (A 4) is substituted. Since  $\phi(1; \phi(0))$  is an analytic function of  $\phi(0)$ , the equality sign in (A 7) may only apply at a finite number of isolated points.

The points  $P_U$  and  $P_S$  for which (6.4) is satisfied are obtained as solutions of the equation

$$\phi(1; \phi(0)) = \phi_0 + 2\pi k. \quad (\text{A } 8)$$

From (A 7), for  $\phi(0) \in \text{arc}AB$ ,  $\phi(1) - \phi(0)$  is a monotonically increasing function of  $\phi(0)$ , except possibly for a finite number of isolated points (where it is non-decreasing). Therefore (A 8) possesses at most a single solution there. Similarly (A 8) may only have a single solution for  $\phi_0 \in \text{arc}\bar{A}\bar{B}$ .

Finally, as regards stability, (A 7) implies that, during each period, each point initially on the arcAB increases its distance from the periodic point  $P_U$ , until it eventually transfers to arc $\bar{A}\bar{B}$ . By the same token, each point on arc $\bar{A}\bar{B}$  approaches closer to  $P_S$  during each period. Thus, the motion of the system eventually converges to the periodic solution of the TPA represented by the point  $P_S$  on the Poincaré map.

## REFERENCES

- ALMOG, Y. & FRANKEL, I. 1995 The motion of axisymmetric dipolar particles in homogeneous shear flows. *J. Fluid Mech.* **289**, 243–261.
- ARNOLD, V. I. 1983 *Geometrical Methods in the Theory of Ordinary Differential Equations*. Springer.
- BACRI, J. C., PERZYNSKI, R., SHLIOMIS, M. I. & BURDE, G. I. 1995 “Negative-viscosity” effect in magnetic fluid. *Phys. Rev. Lett.* **75**, 2128–2131.
- BATCHELOR, G. K. 1970 The stress system in a suspension of force-free particles. *J. Fluid Mech.* **41**, 545–570.
- BENDER, C. M. & ORSZAG, S. A. 1978 *Advanced Mathematical Methods for Scientists and Engineers*. McGraw-Hill.
- BIRKHOFF, G. & ROTA, G.-C. 1962 *Ordinary Differential Equations*. Ginn & Co.
- BOHR, T., BAK, P. & JENSEN, M. H. 1984 Transition to chaos by interaction of resonances in dissipative systems. II. Josephson junctions, charge-density waves, and standard maps. *Phys. Rev. A* **30**, 1970–1981.
- BRENNER, H. 1970a Rheology of two-phase systems. *Ann. Rev. Fluid Mech.* **2**, 137–176.
- BRENNER, H. 1970b Rheology of a dilute suspension of dipolar spherical particles in an external field. *J. Colloid Interface Sci.* **32**, 141–158.
- BRENNER, H. & WEISSMAN, M. H. 1972 Rheology of a dilute suspension of dipolar particles in an external field. II. Effects of rotary Brownian motion. *J. Colloid Interface Sci.* **41**, 499–531.
- CODDINGTON, E. A. & LEVINSON, N. 1955 *Theory of Ordinary Differential Equations*. McGraw-Hill.
- GAZEAU, F., HEEGARD, B. M., BACRI, J.-C., CEBERS, A. & PERZYNSKI, R. 1996 Magnetic fluid under vorticity: Free precession decay of magnetization and optical anisotropy. *Phys. Rev. E* **54**, 1–4.
- GUCKENHEIMER, J. & HOLMES, P. 1983 *Nonlinear Oscillations, Dynamical Systems, and Bifurcation of Vector Fields*. Springer.
- HALL, W. F. & BUSENBERG, S. N. 1969 Viscosity of magnetic suspensions. *J. Chem. Phys.* **51**, 137–144.
- HEEGARD, B. M., BACRI, J.-C., PERZYNSKI, R. & SHLIOMIS, M. I. 1996 Magneto-vortical birefringence in a ferrofluid. *Europhys. Lett.* **34**, 299–304.
- HINCH, E. J. & LEAL, L. G. 1972 Note on the rheology of a dilute suspension of dipolar spheres with weak Brownian couples. *J. Fluid Mech.* **56**, 803–813.
- JONES, M. S., LEBARON, L. & PEDLEY, T. J. 1994 Biflagellate gyrotaxis in a shear flow. *J. Fluid Mech.* **281**, 137–158.
- KUMAR, C. V. A., KUMAR, K. S. & RAMAMOCHAN, T. R. 1995 Chaotic dynamics of periodically forced spheroids in simple shear flow with potential application to particle separation. *Rheol. Acta* **34**, 504–511.
- KUMAR, K. S. & RAMAMOCHAN, T. R. 1995 Chaotic rheological parameters of periodically forced suspensions of slender rods in simple shear flow. *J. Rheol.* **39**, 1229–1241.
- PEDLEY, T. J. & KESSLER, J. O. 1992 Hydrodynamic phenomena in suspensions of swimming microorganisms. *Ann. Rev. Fluid Mech.* **24**, 313–358.
- PUYESKY, I. & FRANKEL, I. 1998 Effects of time-periodic fields on the rheology of suspensions of dipolar spheres. In *Non-Linear Singularities in Deformation and Flow* (ed. D. Durban & A. Pearson) Kluwer (in press).
- RAMAMOCHAN, T. R., SAVITHRI, S., SREENIVASAN, R. & CHANDRA SHEKARA BATH, C. 1994 Chaotic dynamics of a periodically forced slender body in a simple shear flow. *Phys. Lett. A* **190**, 273–278.
- ROSENSWEIG, R. E. 1985 *Ferrohydrodynamics*. Cambridge University Press.
- SHLIOMIS, M. I. & MOROZOV, K. I. 1994 Negative viscosity of ferrofluid under alternating magnetic field. *Phys. Fluids* **6**, 2855–2861.
- STEINBERGER, B., PETERSEN, N., PETERMAN, H. & WEISS, D. G. 1994 Movement of magnetic bacteria in time-varying magnetic fields. *J. Fluid Mech.* **273**, 189–211.
- SZERI, A. J. & LEAL, L. G. 1993 Microstructure suspended in three-dimensional flows. *J. Fluid Mech.* **250**, 143–167.
- SZERI, A. J., MILLIKEN, W. J. & LEAL, L. G. 1992 Rigid particles suspended in time-dependent flows: irregular versus regular motion, disorder versus order. *J. Fluid Mech.* **237**, 33–56.
- SZERI, A. J., WIGGINS, S. & LEAL, L. G. 1991 On the dynamics of suspended microstructure in unsteady, spatially inhomogeneous, two-dimensional fluid flows. *J. Fluid Mech.* **228**, 207–241.